



The influence of ball milling process on hydrogenation properties of $\text{MgH}_2\text{--FeTiH}_x$ composites

Z. Zaranski, T. Czujko*

Faculty of Advanced Technology and Chemistry, Military University of Technology, Kaliskiego 2 St, 00-908 Warsaw, Poland

ARTICLE INFO

Article history:

Received 11 July 2010

Received in revised form 7 October 2010

Accepted 8 October 2010

Available online 23 October 2010

Key words:

Hydrogen storage materials
Nanostructured hydride mixtures
Composites
Desorption kinetics
Ball milling
X-ray diffraction

ABSTRACT

In this work, the $\text{MgH}_2\text{--FeTiH}_x$ composites were synthesized in a wide range of compositions by reactive mechanical milling. The phase structure and morphology were investigated by XRD and SEM. The hydrogen desorption characteristics of obtained composites were measured by a volumetric method using Sievert's apparatus. It is demonstrated that the hydrogen desorption kinetics in the magnesium–intermetallic hydride composites is affected not only by the phase composition but also by the milling parameters. The particle size of composite constituents is slightly related to the amount of additive and strongly to milling time. The exponential factor in Johnson–Mehl–Avrami's equation decreases for composite powders in comparison to reference MgH_2 from ~ 2 to ~ 1 . Our results clearly show that there is a considerable catalytic effect of the FeTi additive on the hydrogen absorption and desorption kinetics. The energy of activation for both processes decreases in visible way for MgH_2 catalyzed by 50 wt.% of FeTiH_x hydride.

© 2010 Elsevier B.V. All rights reserved.

1. Introduction

Magnesium hydride is well-known material which has been considered as a hydrogen storage medium for more than two decades. Unfortunately, large enthalpy of formation and high desorption temperature of the magnesium hydride ($\sim 300^\circ\text{C}$) exclude its usage in practical applications. However, it has been shown that compositing of MgH_2 with some intermetallic alloys can decrease the decomposition temperature of MgH_2 [1–7]. In this case the low temperature hydride counterpart acts as a catalyst which does not decrease dramatically a total capacity of the system.

Recently, we have shown that this composite behavior of hydride mixtures is observed in metal, intermetallic and complex hydride systems [8,9]. In the present work, the composite approach is applied to the $\text{MgH}_2 + \text{FeTiH}_x$ system. The composites with various volume fractions of additive constituent were processed by controlled ball milling (CBM) in a magneto-mill under hydrogen or argon atmosphere. The hydrogenation properties were studied using Sievert's Apparatus and Johnson–Mehl–Avrami's model of phase transformation. The aim of this work is to analyze the influence of composition and milling parameters on hydrogenation properties of $\text{MgH}_2\text{--FeTiH}_x$ composites.

2. Experimental

As-received commercial MgH_2 powder (purchased from Sigma–Aldrich; ~ 98 wt.% purity) and synthesized FeTiH_x hydride powders are mixed to $\text{MgH}_2 + X$ wt.% FeTiH_x compositions, where $X = 10, 30$ and 50 . As a reference MgH_2 without additive was used.

The FeTi intermetallic powder was obtained by melting pre-compressed Fe and Ti powders mixture and grinding the obtained ingot. Ground powder was pre-milled in hydrogen under ~ 700 kPa pressure for 5 h and then mixed with MgH_2 . Mixed powders were milled for 5, 10 and 25 h for composites with 10 and 30 wt.% of FeTi additive and for 5, 10, 25, 50 and 100 h for composite modified by 50 wt.% of FeTi intermetallic powder. In a case of the reference MgH_2 powder continuous Controlled Mechanical Milling (CMM) was carried out for 10 h in hydrogen under ~ 500 kPa pressure in the magneto-mill Uni-Ball-Mill 5 (A.O.C. Scientific Engineering Pty Ltd., Australia), using a high energy shearing mode with two NdFeB external magnets mode. The balls-to-powder weight ratio was ~ 50 and the rotational speed of milling vial was ~ 175 rpm.

Morphological examination of powders was conducted with SEM Philips microscope LaB₆ XL-30. The size measurement of the powder particles for various samples was carried out by attaching loose powder to a sticky carbon tape and taking pictures under SE mode in SEM. The images were analyzed by the Image Tool v.3.00 software. The size of the powders was calculated as the particle equivalent circle diameter (ECD),

$$\text{ECD} = \sqrt{\frac{4 \cdot A}{\pi}} \quad (1)$$

where A represents the projected particle area.

The phase structure of as milled and reference powders was characterized by Seifert powder diffractometer. Monochromated $\text{Co K}\alpha_1$ radiation was used in this study. The scan range was from $2\theta = 20^\circ$ to 130° and the scan rate was $0.6^\circ \text{ min}^{-1}$ at the step size of 0.02° .

The hydrogenation properties were investigated using Sievert's type apparatus at 300 and 325°C under atmospheric pressure of hydrogen for desorption and 25 bars for absorption process. The influence of milling parameters on mechanism and

* Corresponding author. Tel.: +48 022 683 9445; fax: +48 022 683 9445.
E-mail address: tczujko@wat.edu.pl (T. Czujko).

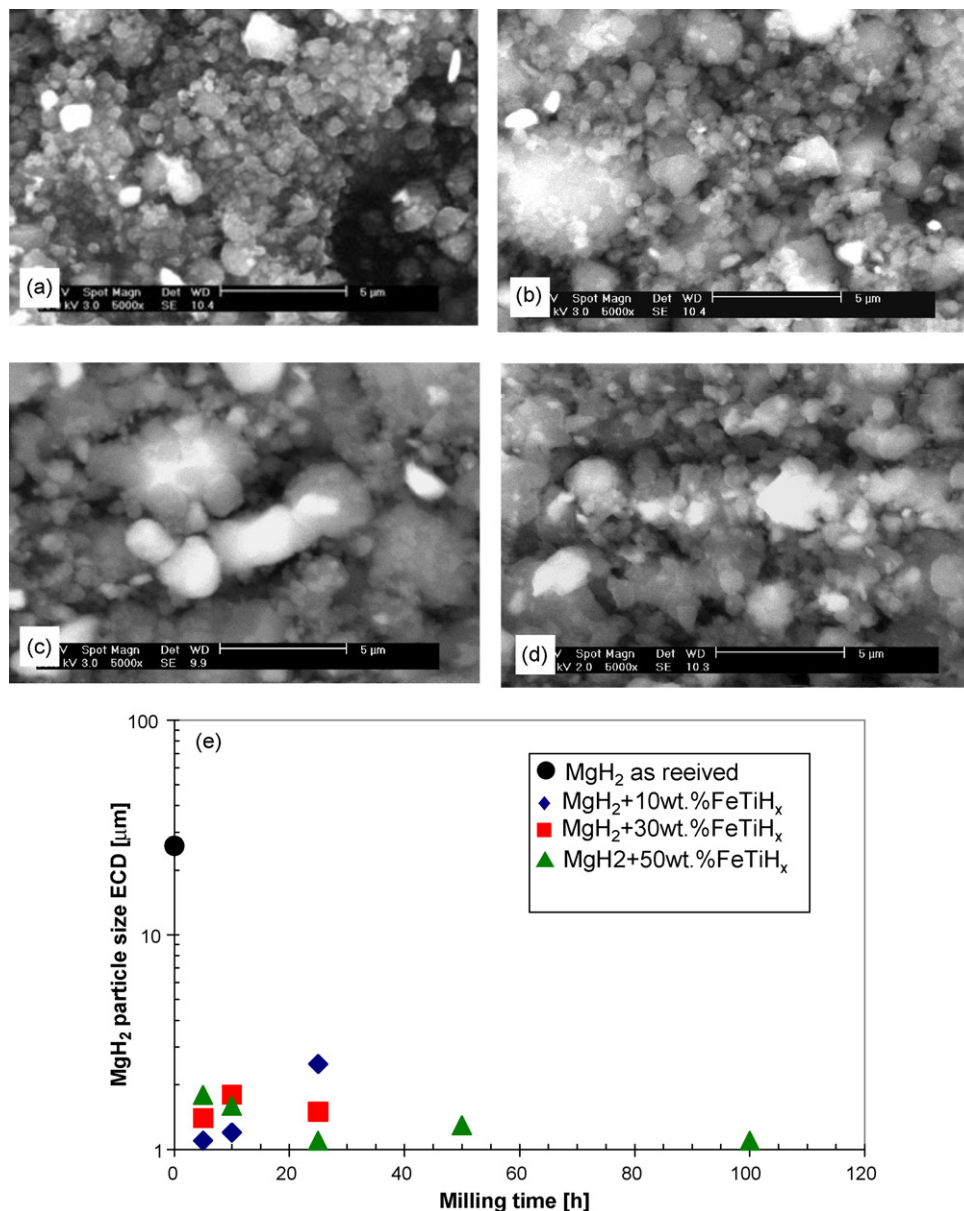


Fig. 1. The morphology of (a) MgH₂ reference powder and MgH₂-FeTiH_x composites after milling for 10 h with (b) 10 wt.% FeTiH_x (c) 30 wt.% FeTiH_x and (d) 50 wt.% FeTiH_x as well as (e) the influence of milling time on particle size of above composite powders.

energy of activation for decomposition and hydride formation processes was studied for MgH₂ + 50 wt.%FeTiH_x composite. The activation energy was estimated from Arrhenius plot of K values with temperature

$$K = K_0 e^{-Q/RT} \quad (2)$$

where Q is the activation energy, R is gas constant and T is the temperature. The rate constant K was determined by fitting the desorption curves with the Johnson-Mehl-Avrami (JMA) equation [10]:

$$\alpha = 1 - e^{-(Kt)^\eta} \quad (3)$$

where η is the reaction exponent and α is the desorption fraction at time t .

3. Results and discussion

3.1. Morphology and structure of MgH₂ + FeTiH_x composites

Fig. 1a–d shows the morphology of reference material (MgH₂ without additives) and the MgH₂ + FeTiH_x composites after 10 h ball milling for 10, 30 and 50 wt.% FeTiH_x. By comparison with as received material (results not presented in this work) it is clearly

seen that ball milling reduced significantly the original particle size of MgH₂ (ECD ~ 38 μm). After milling for 10 h the average particle size is reduced to 1–2 μm. There is no visible influence of FeTiH_x content in various composites on their powders particle size and morphology. The influence of composition and milling time on particle size of MgH₂ powders was presented in Fig. 1e. It shows that even after relatively short milling time (5 h) and regardless to composition a visible particle size reduction is observed. Increasing milling to 100 h does not cause further MgH₂ refining.

Fig. 2 showing the XRD patterns of the 10, 30 and 50 wt.% FeTiH_x composites after milling confirms that the microstructure comprises primarily MgH₂ and FeTi with a small amount of minority intermetallic Fe₂Ti. The formation of Fe₂Ti is related to inhomogeneous structure of ingot obtained during casting process. The lack of diffraction peaks from β-FeTiH₂ or γ-FeTiH phases is mostly related to relatively fast kinetics of decomposition process of both hydrides. Nevertheless, the formation of hydrides based on FeTi intermetallic phase was confirmed by hydrogen pressure drop in mill cylinder

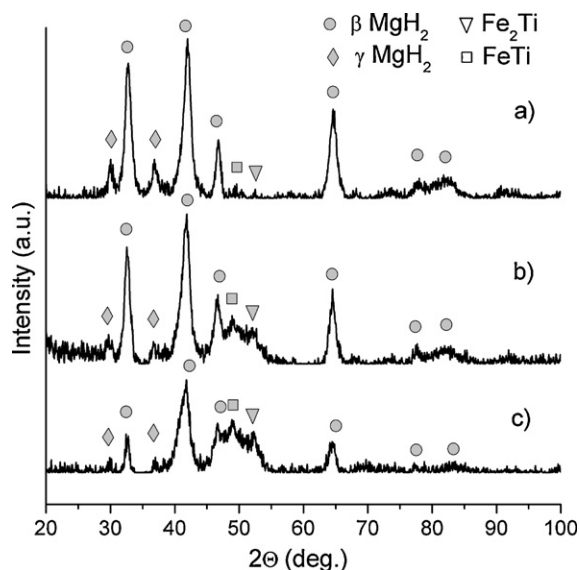


Fig. 2. XRD patterns of $\text{MgH}_2\text{-FeTiH}_x$ composites after milling for 10 h with (a) 10 wt.% FeTiH_x , (b) 30 wt.% FeTiH_x and (c) 50 wt.% FeTiH_x .

Table 1

The value of desorbed and absorbed hydrogen in as received, milled and catalyzed MgH_2 .

Composition/milling time [h]	Desorption at 325 °C [wt.%]					
	0	5	10	25	50	100
MgH_2 as received	0.001	–	–	–	–	–
MgH_2 milled	–	–	7.1	–	–	–
$\text{MgH}_2 + 10 \text{ wt.\% FeTiH}_x$	–	5.4	6.4	6.3	–	–
$\text{MgH}_2 + 30 \text{ wt.\% FeTiH}_x$	–	–	5.5	5.2	–	–
$\text{MgH}_2 + 50 \text{ wt.\% FeTiH}_x$	–	3.8	3.8	3.5	3.1	2.9
Composition/milling time [h]	Absorption at 300 °C [wt.%]					
	0	5	10	25	50	100
MgH_2 as received	0.6	–	–	–	–	–
MgH_2 milled	–	–	6.8	–	–	–
$\text{MgH}_2 + 10 \text{ wt.\% FeTiH}_x$	–	5.2	5.6	5.4	–	–
$\text{MgH}_2 + 30 \text{ wt.\% FeTiH}_x$	–	–	4.4	4.2	–	–
$\text{MgH}_2 + 50 \text{ wt.\% FeTiH}_x$	–	3.9	3.0	2.9	3.5	2.8

during reactive ball milling and has been published in our previous work [11]. On the other hand, milling is well known method of hydride activation [12] and it can improve hydrogenation properties of FeTi phase. It allows us to assume that FeTi intermetallic phase not only will act as a catalytic additive but also will form FeTiH_x hydride which might play the role as composite constituent.

3.2. Hydrogenation properties of $\text{MgH}_2 + \text{FeTiH}_x$ composites

The kinetics curves (Fig. 3) obtained for hydrogen desorption which was carried out at 325 °C and under atmospheric pressure of hydrogen. The as-received MgH_2 which characterizes by large particles and polycrystalline form did not decompose at this temperature what is in agreement with results presented by Huot et al. [12] and Varin et al. [13]. Milling process (reference MgH_2) causing particle size reduction and hydride nanostructurization, in visible way increases hydrogen desorption kinetics. Desorption curve possesses typical sigmoidal shape with relatively short incubation period (~2 min). The value of desorbed hydrogen after 20 min is 7.1 wt.% which is close to the theoretical value of purified magnesium hydride (7.4 wt.%). The proportional capacity decreasing as a function of FeTiH_x content in hydride composites is presented in Table 1.

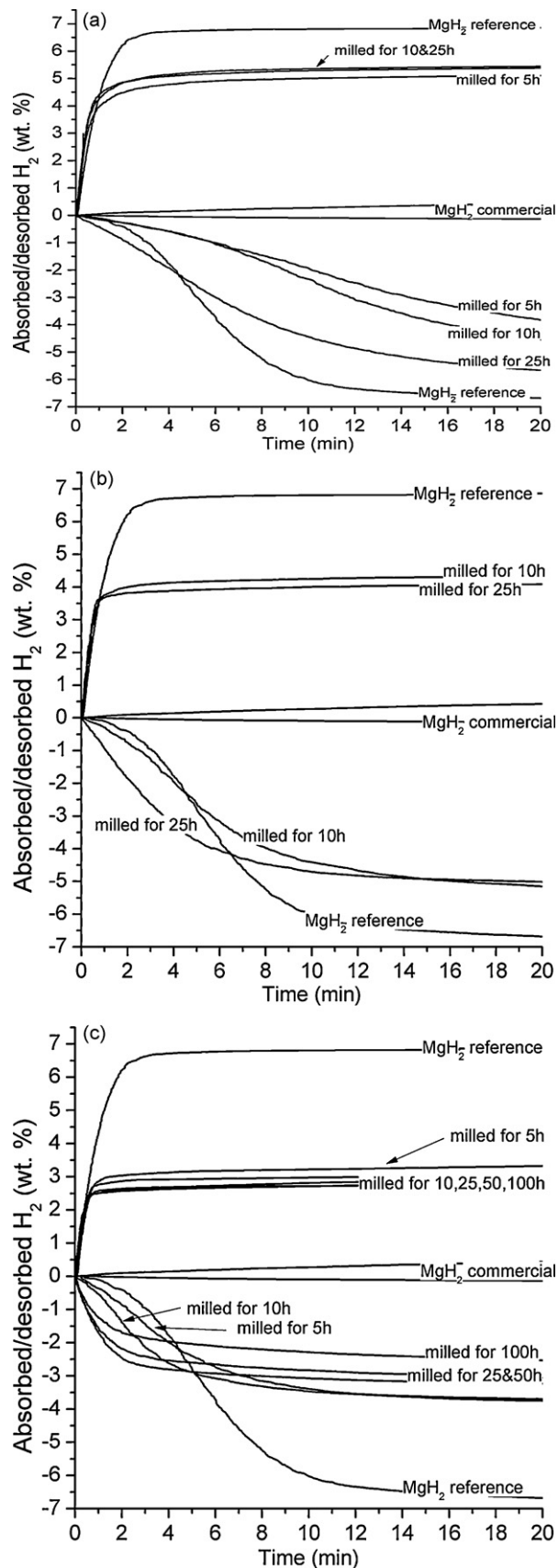


Fig. 3. The absorption and desorption kinetics curves for MgH_2 modified by (a) 10 wt.% FeTiH_x , (b) 30 wt.% FeTiH_x and (c) 50 wt.% FeTiH_x milled for various times in comparison to as received and reference MgH_2 .

Table 2The value of η reaction exponent for reference MgH_2 and composite hydrides.

Composition/milling time [h]	5	10	25	50	100
MgH_2 reference	–	2.1*	–	–	–
$\text{MgH}_2 + 10 \text{ wt.}\% \text{FeTiH}_x$	1.4	1.4	1.3	–	–
$\text{MgH}_2 + 30 \text{ wt.}\% \text{FeTiH}_x$	–	1.6	1.2	–	–
$\text{MgH}_2 + 50 \text{ wt.}\% \text{FeTiH}_x$	1.3	1.0	1.0	0.9	0.8

* Parameter independent on milling time for this particular material [9].

Much less complicated situation was noticed for hydrogen absorption which was obtained at temperature 300°C under 25 bar show effect of milling time and composition influence on reaction kinetics for milled and catalyzed MgH_2 . In the case of as received material practically negligible absorption ($\sim 0.6 \text{ wt.}\%$) was observed (Fig. 3). The absorbed hydrogen amount as a function of milling time and composition is presented in Table 1. It is clear that capacity decreases with increasing of FeTiH_x quantity. For $\text{MgH}_2 + 50 \text{ wt.}\% \text{FeTiH}_x$ composite noticeable dependence between magnesium capacity and milling time was observed. Varin et al. [13] have already reported similar phenomenon for milled MgH_2 . The authors explain this behavior by increasing of volume fraction of grain boundaries which can store much less hydrogen than in grain volume. The increased volume fraction of grain boundaries is related to nanostructurization process caused by long ball milling time.

In the case of composite hydrides slight kinetics improvement was observed with increasing of milling time (Fig. 3). This qualitative observation was confirmed by analysis of reaction exponent η from Johnson–Mehl–Avrami's equation (Eq. (3)) presented in Table 2. This parameter decreases gradually with increased amount of FeTiH_x additive and increased milling time. The influence of milling parameters on mechanism and energy of activation for decomposition and hydride formation processes was studied for $\text{MgH}_2 + 50 \text{ wt.}\% \text{FeTiH}_x$ composite, where the catalytical influence is the most effective.

The reaction exponent decreases from 2 to 1.3 for non-catalyzed reference magnesium hydride and $\text{MgH}_2 + 50 \text{ wt.}\% \text{FeTiH}_x$ composite milled for 5 h, respectively. Moreover, the changes of η parameter for MgH_2 hydride catalyzed by FeTiH_x additive versus milling time, were noticed. The reaction exponent decreased from 1.3 for composite milled for 5 h to 0.8 after 100 h of milling. The different values of η parameter suggest that different mechanisms are rate controlling for various powders. According to Karty et al. [14] the value of ~ 2 suggests that the transformation of $\beta\text{-MgH}_2$ to Mg upon desorption is either diffusion rate limited occurring by two-dimensional growth at constant nucle-

ation rate or alternatively, it is interface-controlled transformation with one-dimensional growth at constant nucleation rate or two-dimensional growth at constant nuclei number. The η value close to 1 suggests either diffusion rate limited transformation occurring by two-dimensional growth at constant nuclei number or alternatively, interface-controlled transformation with one-dimensional growth at constant nuclei number.

The energy of hydrogen desorption estimated using Arrhenius plot (Eq. (2)) amounts to 80 kJ/mol , which is in comparison to energy of activation for milled magnesium hydride (205 kJ/mol) [11] results in great kinetic improvement of catalyzed material.

4. Conclusions

The obtained nanocomposite exhibits a good reversibility. The catalytic element introduced into the system from decomposing an intermetallic hydride, proportionally to catalyst amount reduces the total capacity of the composite system. The milling time increasing and powder composition affects the hydrogen desorption kinetics. The observed energy of activation for catalyzed $\text{MgH}_2 + 50 \text{ wt.}\% \text{FeTiH}_x$ system (80 kJ/mol) characterizes by visible reduction in comparison to only milled MgH_2 (205 kJ/mol).

Acknowledgements

This work was supported by a grant from the State Committee for Scientific Research of Poland (No. N507 352735) which is gratefully acknowledged.

References

- [1] M. Terzieva, M. Khrussanova, P. Peshev, J. Alloys Compd. 267 (1998) 235–239.
- [2] G. Liang, S. Boily, J. Huot, J. Alloys Compd. 268 (1998) 302–307.
- [3] D. Sun, H. Enoki, J. Alloys Compd. 282 (1999) 252–257.
- [4] O.N. Srivastava, D.J. Davidson, S.S. SaiRaman, J. Alloys Compd. 292 (1999) 194–201.
- [5] P. Mandal, O.N. Srivastava, J. Alloys Compd. 205 (1994) 114–118.
- [6] P. Wang, A.M. Wang, B.Z. Ding, Z.Q. Hu, J. Alloys Compd. 334 (2002) 243–248.
- [7] R. Vijay, R. Sundaresan, M.P. Maiya, S. Srinivasa Murthy, Y. Fu, H.-P. Klein, M. Groll, J. Alloys Compd. 384 (2004) 283–295.
- [8] R.A. Varin, T. Czujko, R. Pulz, Z. Wronski, J. Alloys Compd. 483 (2009) 252–255.
- [9] T. Czujko, R.A. Varin, Z.S. Wronski, Z. Zaranski, Can. Metall. Quart. 1 (2009) 11–26.
- [10] M. Avrami, J. Chem. Phys. 7 (1939) 1103.
- [11] T. Czujko, Z. Zaranski, Mater. Eng. 3 (2010) 460–463.
- [12] J. Huot, G. Liang, S. Boily, A. Van Neste, R. Schulz, J. Alloys Compd. 293–295 (1999) 495–500.
- [13] R.A. Varin, T. Czujko, Z.S. Wronski, Nanomaterials for Solid State Hydrogen Storage, Springer Science + Business Media, New York, USA, 2009.
- [14] A. Karty, J. Grunzweig-Genossar, P.S. Rudman, J. Appl. Phys. 50 (1979) 7200–7209.